Ecological Indicators 98 (2019) 80–87

Contents lists available at ScienceDirect

Ecological Indicators

journal homepage: www.elsevier.com/locate/ecolind

Changes in soil organic carbon and microbial carbon storage projected during the 21st century using TRIPLEX-MICROBE

Kefeng Wang[a,b], Changhui Peng[c,b,*], Qiuan Zhu[b], Meng Wang[b], Gangsheng Wang[d], Xiaolu Zhou[c], Yanzheng Yang[e], Juhua Ding[b], Hua Wei[b]

[a] Key Laboratory of Resource Biology and Biotechnology in Western China, Northwest University, Taibai North Road 229, Xi'an, Shaanxi 710069, China
[b] Center for Ecological Forecasting and Global Change, College of Forestry, Northwest A&F University, Yangling, Shaanxi 712100, China
[c] Department of Biological Sciences, Institute of Environmental Sciences, University of Quebec at Montreal, C.P. 8888, Succ. Centre-Ville, Montreal H3C 3P8, Canada
[d] Environmental Sciences Division & Climate Change Science Institute, Oak Ridge National Laboratory, Oak Ridge, TN 37831-6301, USA
[e] Department of Earth System Science, Tsinghua University, Haidaian, Beijing 100084, China

ARTICLE INFO

Keywords:
Soil organic carbon
Microbial carbon
Representative concentration pathways
Climate change
Terrestrial ecosystem model

ABSTRACT

Microbial physiology is very important in the biogeochemical cycles of the Earth system. Considerable uncertainty exists in the responses of global soil organic and microbial carbon to future climate change. In this study, future changes in the global soil organic carbon (SOC) and microbial carbon (MBC) pools are simulated using TRIPLEX-MICROBE, which considers and predicts microbial activity, under three future representative concentration pathways (RCPs) in the 21st century. Between 2013 and 2100, TRIPLEX-MICROBE simulates decreases in SOC from 1099 Pg (petagrams, 10^{12} kg) to 1032 Pg, 996 Pg and 924 Pg under RCP scenarios RCP2.6, RCP4.5 and RCP8.5, respectively, representing reductions of approximately 6.1%, 9.4% and 15.9%, respectively. The MBC reaches a stable state after 2030 under RCP2.6, and it increases from 20.89 Pg to 23.78 Pg between 2013 and 2100. Under RCP4.5 and RCP8.5, MBC increases by 20.3% and 39.6%, respectively, between 2013 and 2100. The SOC stored in the Arctic declines under the priming effect; however, as the climate gradually warms from the equator to the mid-latitudes, the Northern Hemisphere becomes a larger carbon sink, which could offset the carbon losses from high-latitude and high-altitude regions. The latitude where the MBC reaches its maximum during the coldest season of a year in the Northern Hemisphere moves northward approximately 10 degrees under the three RCPs from the latitude in the historical period. Tropical and temperate vegetation expand northward gradually with warming, and vegetation fixes more carbon as it migrates northward to offset the increase in atmospheric CO_2.

1. Introduction

The soil stores the largest amount of carbon in terrestrial ecosystems and plays an important role in the global carbon cycle (Ciais et al., 2013; IPCC, 2014). Changes in soil–atmosphere carbon fluxes may produce important feedbacks on climate over the next century. Soil is considered a sink for atmospheric carbon at present (Quéré et al., 2016); however, the feedback of carbon sinks to climate change remains uncertain (Todd-Brown et al., 2014; Shao et al., 2016). High latitudes contain large amounts of soil carbon (Sistla et al., 2013), and rapidly rising temperatures in the Arctic might produce greater releases of greenhouse gases (GHGs) to the atmosphere (Voigt et al., 2017), forming a strong positive carbon cycle-climate feedback.

Net primary productivity (NPP) is the primary input to soil carbon and is sensitive to climate change. NPP rates vary widely in the terrestrial biosphere, and tropical forests hold a large proportion of total global annual NPP (Cleveland et al., 2013). Elevated temperatures, long growing seasons and increased nutrient availability will alter plant species composition (Chapin et al., 1995) and promote plant growth (Hobbie et al., 2002), especially in the Arctic regions, which are sensitive to climate change. Southern plant communities, such as woody shrubs, will migrate northward (Sistla et al., 2013), and this expansion of shrubs will affect the plant C input to soils (Rousk et al., 2016), inducing a shift from recalcitrant carbon to more labile carbon in the soil profile (Hartley et al., 2012; Rousk et al., 2016).

Soil respiration is a major flux in the global carbon cycle that opposes photosynthetic CO_2 uptake (Mahecha et al., 2010). Soil respiration is expected to increase with rising temperatures, but the degree of

* Corresponding author at: Center for Ecological Forecasting and Global Change, College of Forestry, Northwest A&F University, Yangling, Shaanxi 712100, China.
E-mail address: peng.changhui@uqam.ca (C. Peng).

https://doi.org/10.1016/j.ecolind.2018.10.045
Received 9 June 2018; Received in revised form 12 September 2018; Accepted 21 October 2018
Available online 31 October 2018
1470-160X/ © 2018 Elsevier Ltd. All rights reserved.

response may depend on soil environmental factors (Reynolds et al., 2015). SOC changes are determined based on NPP and soil respiration. Todd-Brown et al. (2014) found that most Earth system models (ESMs) represent permafrost dynamics poorly and omit potential constraints on SOC storage, such as the priming effect, which is defined as an increase or decrease of SOM in response to the input of exogenous carbon sources (Kuzyakov, 2010). SOC can be preserved due to freezing temperatures or high moisture content (e.g., in high-latitude and water-saturated soils) in a range of ecosystems (Trumbore, 2009).

Microbial communities underpin the biogeochemical cycles between atmosphere, soil and ocean (Widder et al., 2016). Microbial physiology is vital to the Earth system (Schimel, 2013). Microbial decomposition of SOC produces a major flux of CO_2 from terrestrial ecosystems and acts as a critical feedback on climate change (Suseela et al., 2012). Temperature is a primary factor in shaping the soil microbial community (Zhou et al., 2016). Elevated temperatures accelerate microbial processes and increase nutrient availability, resulting in higher heterotrophic respiration rates and increased CO_2 releases to the atmosphere (Dorrepaal et al., 2009; Voigt et al., 2017). In a warming environment, limitations imposed by abiotic factors (such as freezing water) on microbial activity may be alleviated in permafrost regions, causing large amounts of SOC to become vulnerable to mineralization (Bradford, 2013).

Representative concentration pathways (RCPs) are four GHGs concentration trajectories adopted by the Intergovernmental Panel on Climate Change (IPCC) for its fifth Assessment Report (AR5) in 2014 (IPCC, 2014). Our analyses are conducted with historical data and three future scenarios: RCP2.6, RCP4.5 and RCP8.5. RCP2.6 assumes that global annual GHG emissions (measured in CO_2-equivalent concentration levels (in ppm)) peak at 490 ppm, with emissions declining substantially thereafter. Under RCP4.5, emissions peak at 650 ppm and then stabilize. Under RCP8.5, emissions continue to rise throughout the 21st century (Moss et al., 2010).

ESMs are essential tools for studying the global carbon cycle and its effects on future climate change (Lawrence et al., 2009). Consideration of microorganisms in ESMs could result in improved simulations of global SOC and predictions of the impacts of future climate change on MBC decomposition and feedback modes (Luo et al., 2015; Bradford et al., 2016). In this study, we use TRIPLEX-MICROBE (Wang et al., 2017), a land ecosystem model based on the Integrated Biosphere Simulator (IBIS) (Foley et al., 1996; Kucharik et al., 2000) and TRIPLEX-GHG (Zhu et al., 2014; Zhu et al., 2015) coupled with the microbial-enzyme-mediated decomposition (MEND) model (Wang et al., 2013; Wang et al., 2015), to simulate global SOC and MBC variations under various climate change scenarios. The objectives of this study are 1) to use TRIPLEX-MICROBE to simulate variations in global NPP and soil heterotrophic respiration (S_{HR}) over the 21st century, 2) to use TRIPLEX-MICROBE to simulate changes in both SOC and MBC over the same period, 3) to quantify the latitudinal changes in soil microbial carbon and long-term carbon storage under future climate change scenarios, and 4) to explore the roles of vegetation and plant-soil-microbe ecosystems in countering global warming.

2. Methods and data

2.1. Description of TRIPLEX-MICROBE

The TRIPLEX-MICROBE model (Wang et al., 2017) couples the TRIPLEX-GHG (Zhu et al., 2014; Zhu et al., 2015) and MEND models (Wang et al., 2013; Wang et al., 2015). The TRIPLEX-GHG model is based on the IBIS, which is coupled with a new methane (CH_4) biogeochemistry module that incorporates CH_4 production, oxidation, and transportation processes and a water table module. The MEND model is based on Michaelis–Menten kinetics and describes the dynamics of physically defined SOC pools. The TRIPLEX-MICROBE model includes seven main modules, namely, the plant phenology, vegetation dynamics, land surface, methanogenesis, water table, microbe (MEND) and soil biogeochemistry modules. TRIPLEX-GHG (and other traditional soil carbon models) is based on fast/slow/passive pools, which are empirically determined and are lacking in key microbial processes that control the soil carbon responses to global climate change (Wang et al., 2013). The novel ecosystem process model TRIPLEX-MICROBE offers considerable improvement over TRIPLEX-GHG by integrating key microbial processes into soil carbon cycles. Details of the structures and features of the models mentioned above are provided in Appendix S1 in Supporting Information and in the studies of Zhu et al. (2014) and Wang et al. (2017).

2.2. Input data

Here, we employ historical (1901–2012) and future (2013–2100) simulations obtained from Phase 5 of the Climate Model Intercomparison Project (CMIP5). These simulations were performed using the IPSL-CM5A-LR ESM and RCP2.6, RCP4.5 and RCP8.5 (Taylor et al., 2012). The monthly climate input data for the historical simulations were obtained from version 3.1 of the Climatic Research Unit time-series climate database (CRU-TS 3.1; http://badc.nerc.ac.uk/data/cru). The selected variables include cloud cover, temperature, diurnal temperature range, precipitation and relative humidity. The other input variables, such as soil type, vegetation, soil properties (texture, pH, and soil carbon), topography and the area of each grid cell, were obtained from the same datasets employed by Zhu et al. (2014). To obtain input data for the future scenarios based on RCP2.6, RCP4.5 and RCP8.5, we selected the output from the IPSL-CM5A-LR ESM (http://cmip-pcmdi.llnl.gov/cmip5/), which was regridded to a resolution of $0.5 \times 0.5^{\circ}$.

To generate a set of input data from 2013 to 2100, we first determine the changes in cloud cover, temperature, diurnal temperature range, precipitation and relative humidity through subtracting the climatological averages of these variables for 1960–2012 from their monthly values from 2013 to 2100 as simulated using IPSL-CM5A-LR driven by RCP2.6, RCP4.5, and RCP8.5. We then add the averages of the historical data from CRU for 1960–2012. Finally, the historical data from CRU that cover 1901–2012 and the values for 2013–2100 from the RCPs are integrated to produce a set of input data that cover the period from 1901 to 2100 for RCP2.6, RCP4.5 and RCP8.5. The data (including climate data, NPP, S_{HR}, SOC and MBC) processing and graphing are performed using R version 3.3.0 (The-R-Core-Team, 2016).

3. Results

3.1. Changes in vegetation type, NPP and soil heterotrophic respiration (S_{HR})

Fig. 1 shows that the vegetation types in the Northern Hemisphere display a pronounced tendency to move northward. Moreover, the degree of northward movement increases from RCP2.6 to RCP8.5. Under RCP8.5, nearly all of northern Canada, northern Russia and Siberia are covered by forests in 2100.

As shown in Fig. 2, NPP and S_{HR} increase with time under the three RCPs from 2001 to 2100. However, under RCP2.6 and RCP4.5, NPP is greater than S_{HR}, which indicates that the land soil carbon pool acts as a carbon sink after 2050. During the same period, NPP is less than S_{HR} under RCP8.5; thus, the terrestrial ecosystem acts as a carbon source under this scenario. NPP and S_{HR} largely stop increasing after 2075 under RCP8.5.

To refine the analysis, the NPP and S_{HR} values are grouped into 5-degree latitude bins from 90°N to 60°S. We find that the changes in NPP and S_{HR} from 90°N to 75°N, 75°N to 60°N, 60°N to 45°N, and 35°S to 60°S are consistent with each 5-degree bin; thus, we analyze the trends by integrating these areas. For 35°N to 45°S, we analyze the trends in NPP and S_{HR} every 5 degrees.

As Fig. 3 shows, S_{HR} is significantly greater than NPP between 90°N

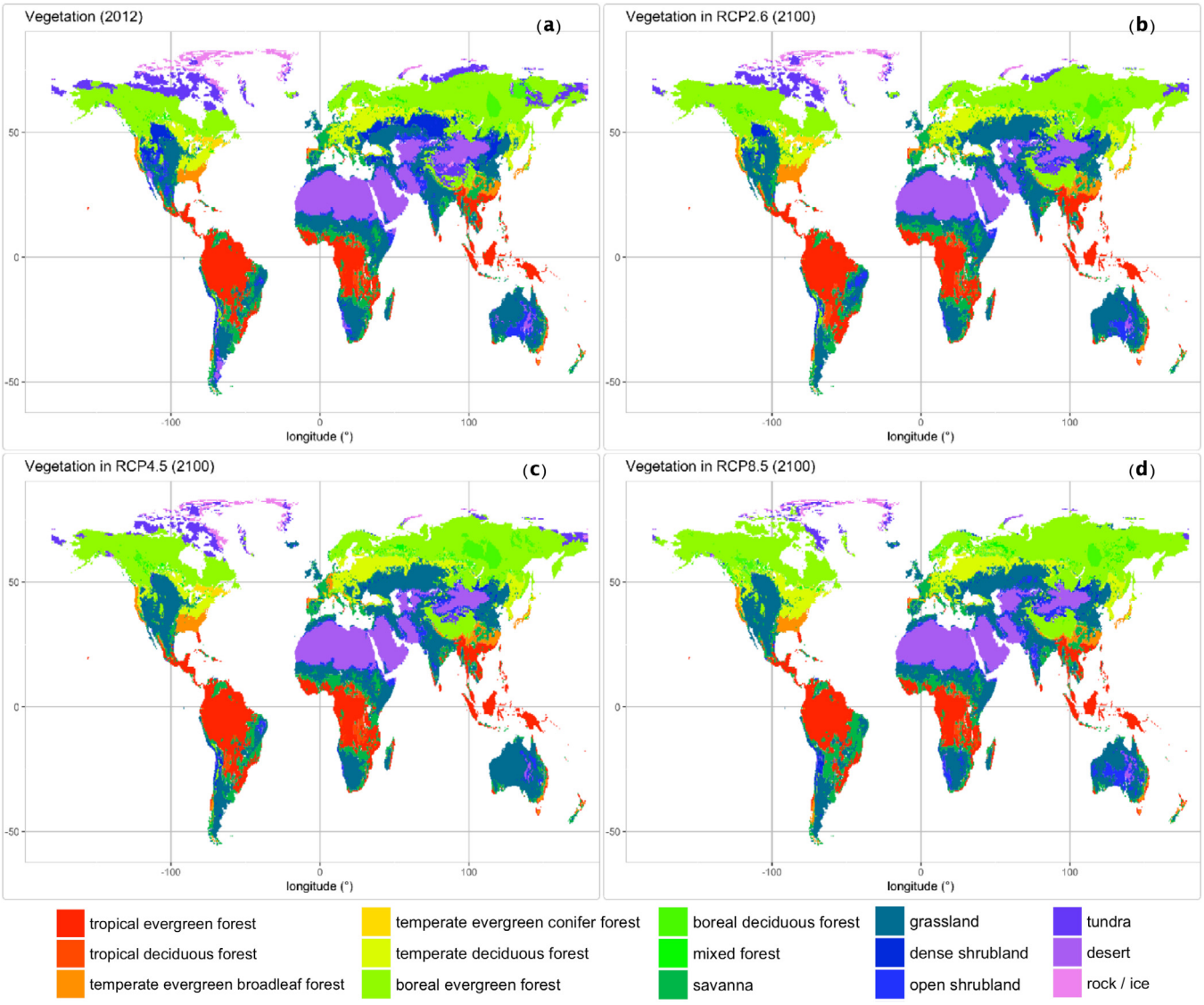

Fig. 1. Vegetation maps simulated by TRIPLEX-MICROBE under the three RCPs. (a) The distribution of vegetation types in 2012; (b) the distribution of vegetation types under RCP2.6 in 2100; (c) the distribution of vegetation types under RCP4.5 in 2100; (d) the distribution of vegetation types under RCP8.5 in 2100.

and 60°N under the three RCPs; moreover, S_{HR} is greater than NPP between 60°N and 45°N under RCP8.5. These results suggest that these regions represent carbon sources in the corresponding RCPs. The SOC estimated by TRIPLEX-MICROBE between 90°N and 45°N accounts for approximately 39% of the total, indicating that the soil organic carbon in this area plays an important role in the global carbon cycle. S_{HR} is less than or equal to NPP, indicating a soil carbon sink, between 45°N and 60°S under the three RCPs. We find that the areas where NPP and S_{HR} stop increasing after 2075 under RCP8.5 are mainly concentrated between 40°N and 30°S.

3.2. Changes in soil organic carbon (SOC)

As shown in Fig. 4, we estimate SOC using the TRIPLEX-MICROBE model under the three RCPs. We find that SOC begins to increase in 2060 and 2075 under RCP2.6 and RCP4.5, respectively. In contrast, the results for RCP8.5 reveal a consistent declining trend in global soil carbon. Between 2013 and 2100, SOC decreases from 1099 Pg to 1032 Pg, 996 Pg and 924 Pg under RCP2.6, RCP4.5 and RCP8.5, respectively; these decreases correspond to 6.1%, 9.4% and 15.9% of the value in 2013, respectively.

As shown in Fig. 5, we analyze the rapid decline in SOC between 2013 and 2050 under the three RCPs using the latitude bins. SOC declines continuously from 90°N to 45°N, and the SOC within this latitude range plays an important role in global change. SOC decreases rapidly and then increases gradually under RCP2.6 and RCP4.5 between 45°N and 30°N, whereas it declines continuously under RCP8.5. SOC displays a continuous increasing trend under the three RCPs from 30°N to 15°S, indicating the presence of a soil carbon sink in these regions.

3.3. Changes in microbial carbon (MBC)

As shown in Fig. 6, we estimate MBC using TRIPLEX-MICROBE under the three RCPs. MBC reaches a stable state after 2030 under RCP2.6, and it increases from 20.89 Pg to 23.78 Pg between 2013 and 2100. Under both RCP4.5 and RCP8.5, MBC shows an overall increasing trend (increasing by 20.3% and 39.6%, respectively) from 2013 to 2100.

The microbial quantity increases significantly at high latitudes (Fig. 7) under RCP8.5. Under both RCP2.6 and RCP4.5, MBC shows downward trends from 90°N to 75°N and from the equator to 5°S and a slowly increasing trend between 20°N and 10°N. Under RCP8.5, MBC shows a significantly increasing trend from 75°N to 40°N and slowly increasing trends from 20°N to 5°N and from 5°S to 15°S. In other areas,

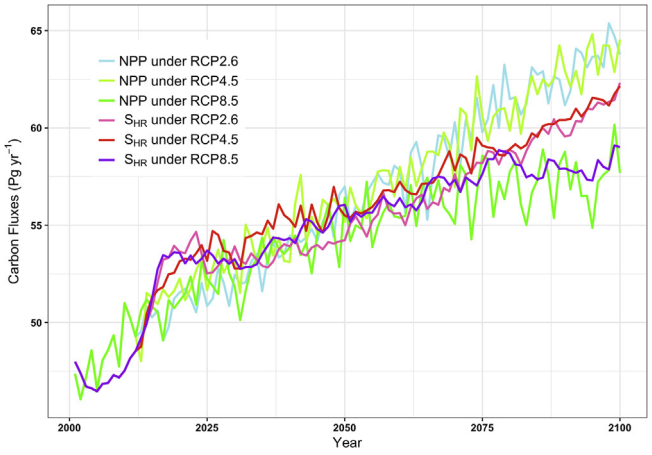

Fig. 2. Annual variations in global NPP and soil heterotrophic respiration (S_{HR}) simulated by TRIPLEX-MICROBE under the three RCPs from 2001 to 2100. "NPP under RCP2.6" denotes the global NPP changes from 2001 to 2100 under RCP2.6; "S_{HR} under RCP2.6" denotes the global S_{HR} changes from 2001 to 2100 under RCP2.6; and the other legend labels, "NPP under RCP4.5," "NPP under RCP8.5," "S_{HR} under RCP4.5," and "S_{HR} under RCP8.5," are expressed in a similar manner.

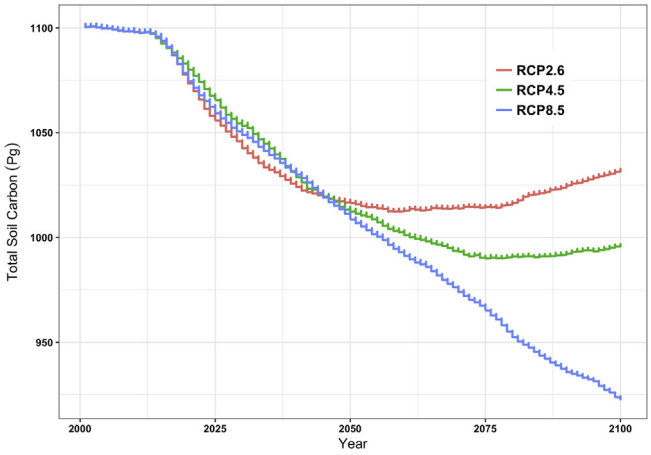

Fig. 4. Annual variations in global SOC simulated by TRIPLEX-MICROBE under the three RCPs from 2001 to 2100.

MBC reaches a dynamic equilibrium under the three RCPs.

We analyze the average global soil MBC density during the historical period (from 2003 to 2012) and the future (from 2091 to 2100 under the three RCPs) simulated by TRIPLEX-MICROBE for the different latitudinal zones (Fig. 8). The MBC density in the future is higher than in the historical period in almost all regions. The microbial biomass clearly varies seasonally. As the radiation intensity increases, delays in the month in which the soil microbial density reaches its maximum occur. For example, the maximum soil MBC density between 90°N and 75°N occurs in June in the historical period; however, it occurs in September under RCP2.6 and RCP4.5 and in October under RCP8.5. The other regions display similar trends.

There is a very interesting phenomenon in the latitudinal MBC densities: The amount of microbial carbon displays reversions at approximately 30°N, near the equator and at 25°S. The MBC density gradually reaches its maximum in the coldest month in each hemisphere at 30°N in December and 25°S in June, and it shows an opposite seasonal pattern on both sides of the equator during the historical period. However, in the last ten years of the 21st century under the three RCPs, the MBC density reaches its maximum in the coldest month, December, near 40°N. This adjustment corresponds to a northward movement of approximately 10 degrees.

Finally, we analyze the average historical (2012) and future (2100; under the three RCPs) global soil MBC densities simulated by TRIPLEX-MICROBE in the different latitudinal zones (Fig. 9). The soil MBC density varies significantly near 60°N between the historical period and each of the three different RCPs. This result shows that the SOC and MBC in this area are very sensitive to latitude-induced climate change.

4. Discussion

4.1. Sink or source of SOC

Approximately 60 Pg of CO_2 are released to the atmosphere through the microbial decomposition of SOC each year (Ågren, 2010). Under climate change, the magnitude of terrestrial carbon will be determined

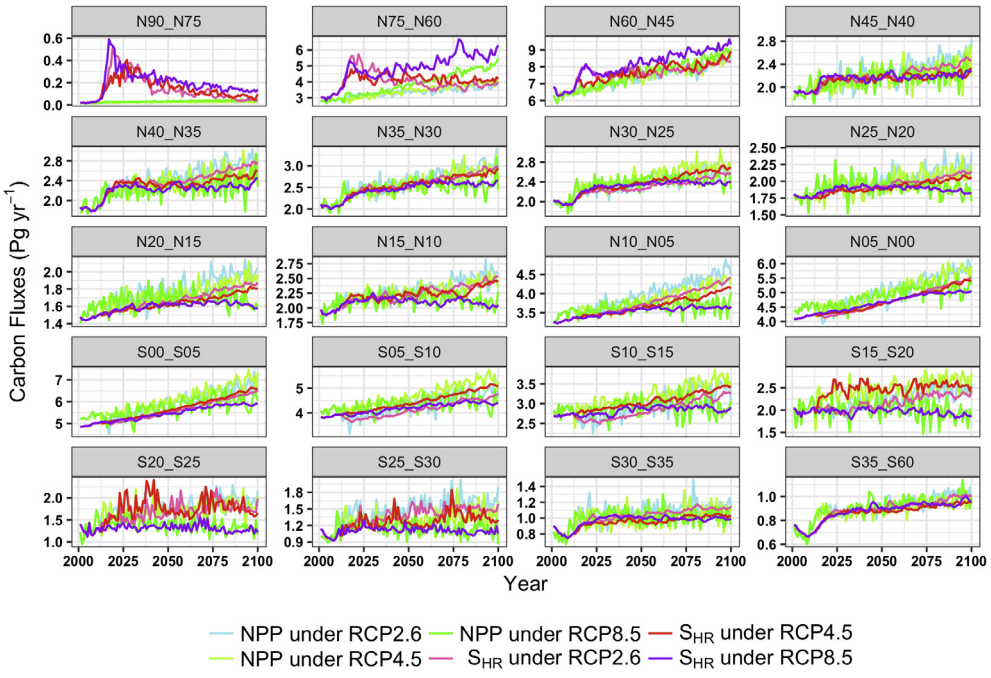

Fig. 3. Annual variations in global NPP and S_{HR} simulated by TRIPLEX-MICROBE within different latitude ranges under the three RCPs from 2001 to 2100. "NPP under RCP2.6" denotes the global NPP changes from 2001 to 2100 under RCP2.6; "S_{HR} under RCP2.6" denotes the global S_{HR} changes from 2001 to 2100 under RCP2.6; and the other legend labels, "NPP under RCP4.5," "NPP under RCP8.5," "S_{HR} under RCP4.5," and "S_{HR} under RCP8.5," are expressed in a similar manner. N90_N75 denotes the range of latitudes extending from 90°N to 75°N, and the other latitude ranges are expressed in a similar manner.

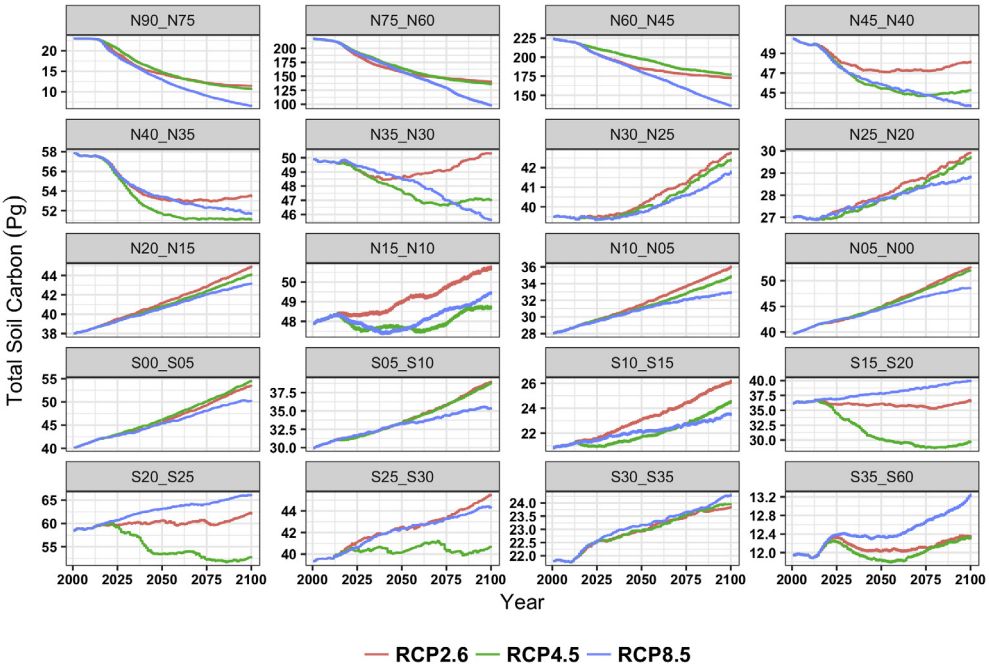

Fig. 5. Annual variations in global SOC simulated by TRIPLEX-MICROBE within different latitude ranges under the three RCPs from 2001 to 2100. N90_N75 denotes the range of latitudes extending from 90°N to 75°N, and the other latitude ranges are expressed in a similar manner.

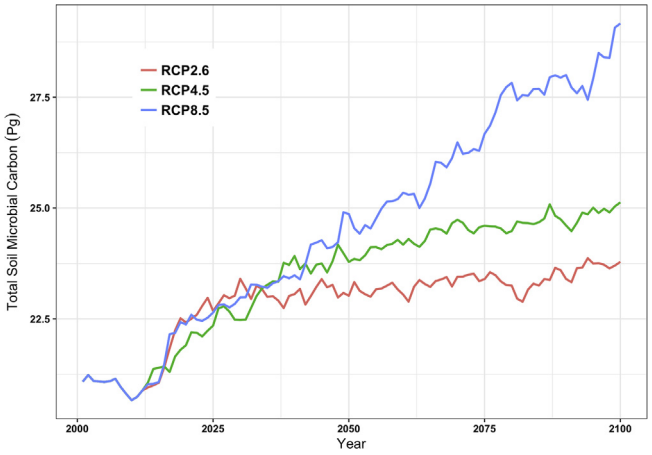

Fig. 6. Annual variations in global soil MBC simulated by TRIPLEX-MICROBE under the three RCPs from 2001 to 2100.

by the interactions among soil microbes, the soil environment and vegetation (Wieder, 2014). The temperature sensitivity at northern latitudes is greater than that at latitudes farther south, suggesting an increased vulnerability of the Arctic region to climate change (Kramshoj et al., 2016). As seen from Fig. 5, SOC in the high Arctic declines rapidly from 2001 to 2100. This result is consistent with recent research (Dorrepaal et al., 2009; Voigt et al., 2017). In contrast, in subtropical to tropical regions and the Southern Hemisphere, SOC mostly displays steady increases. Examination of Fig. 4 reveals that from 2001 to 2100 under RCP8.5, SOC declines north of 30°N, whereas it increases between 30°N and 60°S. The increase in SOC from 30°N to 60°S does not offset the loss that occurs from 90°N to 30°N. Several studies have shown that elevated CO_2 may increase carbon losses from ecosystems by stimulating the decomposition of SOC and may increase the decomposition of soil organic matter (Gill et al., 2002; Lichter et al., 2005; Trueman & Gonzalez-Meler, 2005; Hoosbeek et al., 2006). In Arctic regions, SOC responds more sensitively to temperature increases than it does in temperate and tropical regions. SOC displays accelerated decomposition in the Arctic, primarily due to the effects of microbial priming, which occurs in response to global warming and temperature increases. The SOC at high northern latitudes decreases from 2001 to 2100 (Fig. 5), and soil respiration in the Arctic region (Fig. 3) displays a rapid increase and then decreases gradually. These patterns may be due to the microbial priming effect.

Todd-Brown et al. (2014) compared 11 ESMs for the historical period and RCP8.5, which is associated with high radiative forcing, between 1850 and 2100. Large accumulations of SOC at high latitudes were simulated by many of the ESMs, inconsistent with empirical studies (Todd-Brown et al., 2014). In contrast, TRIPLEX-MICROBE, which considers microbial activity, simulates a decreasing trend in SOC in the Arctic (Fig. 5). The sensitivity of SOC to environmental change represents a critical uncertainty in terrestrial ecosystem models (Sulman et al., 2014). Wieder et al. (2013) integrated microbial activity into the Community Earth System Model (CESM). When microbial communities adapt to increasing temperatures with a constant microbe use efficiency for SOC, RCP8.5 in Fig. 4 displays a similar trend as the simulations performed using CESM and RCP8.5 (Wieder et al., 2013).

NPP generally increases with CO_2, which in turn provides increased carbon inputs to soil (Korner, 2006), although NPP may be constrained by available nutrients (Hungate et al., 2009; Norby et al., 2010). However, several experiments have confirmed that observed increases in NPP do not significantly increase SOC (Hofmockel et al., 2011; Phillips et al., 2012), perhaps because microorganisms in large quantities near the rhizosphere preferentially decompose the fresh NPP derived from litter and/or root exudates in the soil (Wieder, 2014) or because of the short timescale of the experiments relative to SOC turnover times (Billings et al., 2010). Cotrufo et al. (2013) proposed a Microbial Efficiency-Matrix Stabilization (MEMS) framework in which labile plant inputs form stable soil organic matter. This framework considers that labile plant constituents are the dominant source of microbial products (Cotrufo et al., 2013). In response to global warming, microbes exert a priming effect, thus accelerating decomposition and synthesizing protected soil organic matter, such as humus, at the same time. Sulman et al. (2014) showed that the stabilization of 'new' carbon may equal or exceed microbial priming of 'old' SOC in ecosystems with readily decomposable litter (Sulman et al., 2014). These observations from past studies can perhaps explain why SOC continues to increase in

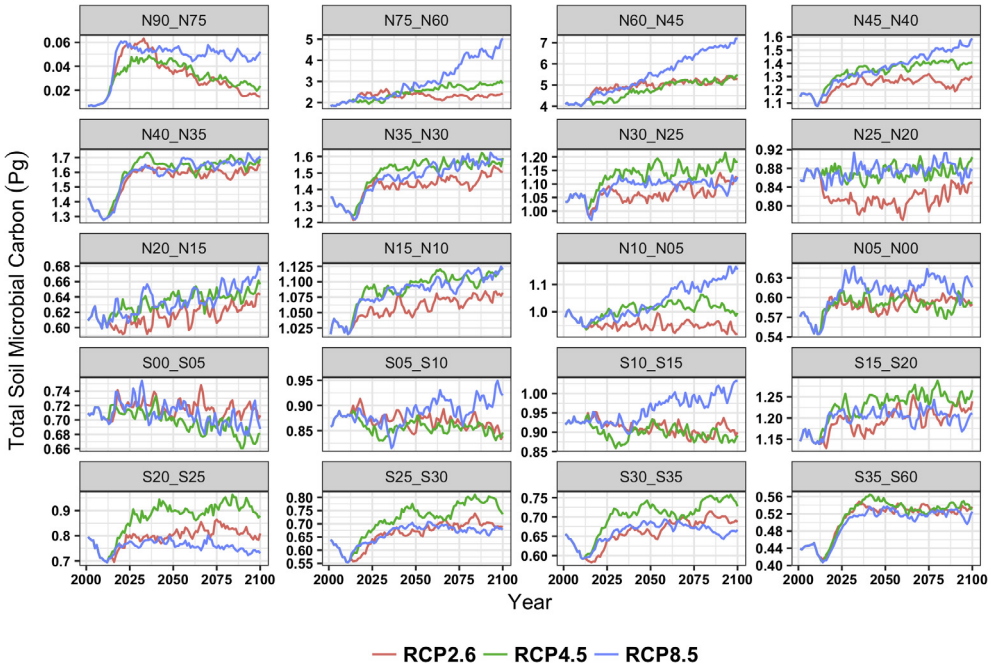

Fig. 7. Annual variations in global MBC simulated by TRIPLEX-MICROBE within different latitude ranges under the three RCPs from 2001 to 2100. N90_N75 denotes the range of latitudes extending from 90°N to 75°N, and the other latitude ranges are expressed in a similar manner.

subtropical and/or tropical areas under the three RCPs in the 21st century in our model, TRIPLEX-MICROBE.

4.2. MBC

Elevated CO_2 levels increase the microbial utilization of soil organic matter (Carney et al., 2007). To a large extent, the Earth system is a product of microbial activity, which is almost invisible in computer simulations of the Earth system (Schimel, 2013). Fig. 8 illustrates how the global MBC changes over the course of a year (i.e., the monthly mean global MBC) during the historical period (2003–2012) and under the three RCPs scenarios (2091–2100). The time when the MBC reaches its maximum occurs later under the three RCPs than during the historical period, likely due to the increases in temperature that occur at high latitudes in the 21st century. The latitude at which the MBC reaches its maximum in the coldest season of the year under the three RCPs (40°N in Fig. 8) in the Northern Hemisphere shows a northward movement of approximately 10 degrees from the corresponding latitude in the historical period (30°N in Fig. 8). This phenomenon ("reversion") may be caused by the seasonal pattern of the revolution of the Earth, in which the amount of sunlight reaching the northern and southern tropics varies. Although we have not identified the specific mechanism responsible for this change, this finding demonstrates that temperature has a strong influence on microorganisms.

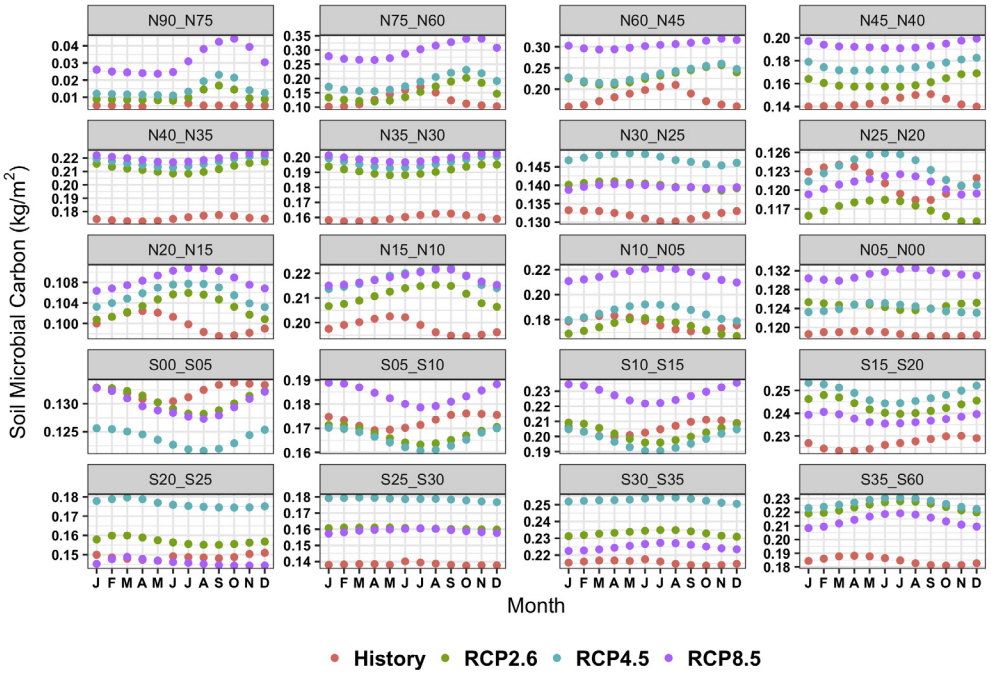

Fig. 8. Monthly variations in soil MBC density simulated by TRIPLEX-MICROBE within different latitude ranges during the historical period and under the three RCPs. Here, "History" denotes the average monthly MBC density between 2003 and 2012, and "RCP2.6," "RCP4.5" and "RCP8.5" denote the average monthly MBC densities between 2091 and 2100 under RCP2.6, RCP4.5 and RCP8.5, respectively. N90_N75 denotes the range of latitudes extending from 90°N to 75°N, and the other latitude ranges are expressed in a similar manner.

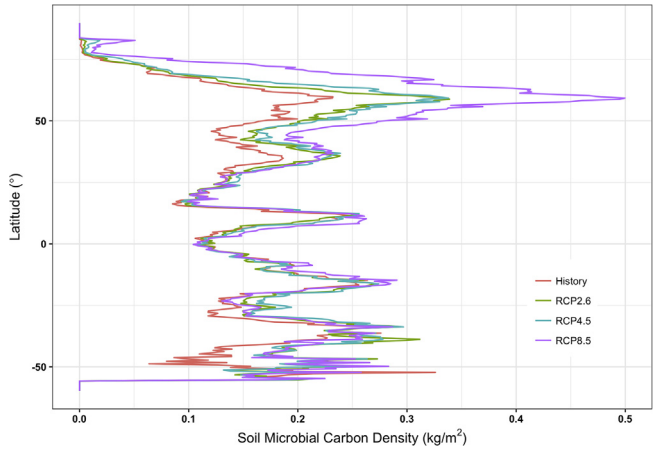

Fig. 9. Latitude variations in soil MBC simulated by TRIPLEX-MICROBE during the historical period and under the three RCPs. Here, "History" denotes the average soil MBC in 2010, and "RCP2.6," "RCP4.5" and "RCP8.5" denote the average soil MBC simulated by TRIPLEX-MICROBE in 2100 under RCP2.6, RCP4.5 and RCP8.5, respectively.

As shown in Fig. 7, the MBC initially displays a rapid increase and then decreases from 90°N to 75°N under the three RCPs through accelerated decomposition or the priming effect of microorganisms, and it is stable or displays a slowly increasing trend in the Northern Hemisphere. As temperature increases, the SOC stored above the Arctic Circle is rapidly released under the priming effect, and the microbial quantity increases dramatically. Subsequently, due to the consumption of soil organic carbon and the adaptation of microorganisms to the increased temperatures, the microbial quantity gradually decreases. As we observe in Fig. 9, the MBC is sensitive to climate warming from 70°N to 50°N because of the magnitude of SOC, especially under RCP8.5.

4.3. Limitations and uncertainties

The main vegetation type in the Arctic, moss, will be replaced by shrubs or coniferous forests under global warming (Shi et al., 2015; Rousk et al., 2016). As shown in Fig. 1, tropical and temperate vegetation gradually expand northward with warming. This expansion leads to further changes in soil structure and soil type, thereby producing changes in SOC. SOC increases from the equator to the poles as the vegetation changes (Fig. 5). Vegetation fixes more carbon as it gradually moves northward to offset the increases in atmospheric CO_2. We speculate that vegetation-soil-microbe ecosystems rather than vegetation alone regulate the responses to global climate warming.

The MICROBE module used in this study has several limitations and uncertainties. It does not consider vertically resolved soil layers or the effects of CO_2 fertilization and fires on SOC and MBC. In addition, the carbon-nutrient coupled MICROBE module is still under development and has not been officially released yet. We suggest that a coupled version of the MICROBE module that considers both C and nutrients would improve the modeled estimates of SOC and MBC in areas that experience nutrient-limiting conditions in the future.

5. Summary and conclusions

In this study, we simulate global SOC and MBC variations in the 21st century using the TRIPLEX-MICROBE model, which considers microbial activity, under three RCPs. Global SOC displays a rapid decline under the three RCPs, which corresponds to 6.1%, 9.4% and 15.9%, respectively, of the value in 2013. This result occurs primarily because the rapid decomposition of carbon in the Arctic is not sufficient to offset the increase in SOC that occurs in temperate and tropical regions (Fig. 5). Global MBC increases by 13.8%, 20.3% and 39.6% between 2013 and 2100 under the three RCPs, and the increase is especially evident under RCP8.5. The latitude at which MBC reaches its maximum during the coldest season of the year in the Northern Hemisphere moves northward approximately 10 degrees under the three RCPs relative to the corresponding latitude in the historical period (Fig. 8). Areas of tropical and temperate vegetation gradually expand northward along with the increase of radiation intensity.

Acknowledgements

This study was partly funded by the National Basic Research Program of China (2013CB956602), the National Science Foundation of China (41571081), a discovery grant from the Natural Sciences and Engineering Research Council of Canada (NSERC) and the QianRen Program of China.

Appendix A. Supplementary data

Supplementary data to this article can be found online at https://doi.org/10.1016/j.ecolind.2018.10.045.

References

Ågren, G.I., 2010. Climate change: microbial mitigation. Nat. Geosci. 3 (5), 303–304. https://doi.org/10.1038/ngeo857.
Billings, S.A., Lichter, J., Ziegler, S.E., Hungate, B.A., Richter, D.D., 2010. A call to investigate drivers of soil organic matter retention vs. mineralization in a high CO2 world. Soil Biol. Biochem. 42 (4), 665–668. https://doi.org/10.1016/j.soilbio.2010.01.002.
Bradford, M.A., 2013. Thermal adaptation of decomposer communities in warming soils. Front. Microbiol. 4. https://doi.org/10.3389/fmicb.2013.00333.
Bradford, M.A., Wieder, W.R., Bonan, G.B., Fierer, N., Raymond, P.A., Crowther, T.W., 2016. Managing uncertainty in soil carbon feedbacks to climate change. Nat. Clim. Change 6 (8), 751–758. https://doi.org/10.1038/nclimate3071.
Carney, K.M., Hungate, B.A., Drake, B.G., Megonigal, J.P., 2007. Altered soil microbial community at elevated CO2 leads to loss of soil carbon. Proc. Natl. Acad. Sci. U.S.A. 104 (12), 4990–4995. https://doi.org/10.1073/pnas.0610045104.
Chapin, F.S.I., Shaver, G.R., Giblin, A.E., Nadelhoffer, K.J., Laundre, J.A., 1995. Responses of arctic tundra to experimental and observed changes in climate. Ecology 694–711 Medium: X; Size.
Ciais, P., Gasser, T., Paris, J.D., Caldeira, K., Raupach, M.R., Canadell, J.G., et al., 2013. Attributing the increase in atmospheric CO2 to emitters and absorbers. Nat. Clim. Change 3 (10), 926–930. https://doi.org/10.1038/Nclimate1942.
Cleveland, C.C., Houlton, B.Z., Smith, W.K., Marklein, A.R., Reed, S.C., Parton, W., et al., 2013. Patterns of new versus recycled primary production in the terrestrial biosphere. Proc. Natl. Acad. Sci. U.S.A. 110 (31), 12733–12737. https://doi.org/10.1073/pnas.1302768110.
Cotrufo, M.F., Wallenstein, M.D., Boot, C.M., Denef, K., Paul, E., 2013. The Microbial Efficiency-Matrix Stabilization (MEMS) framework integrates plant litter decomposition with soil organic matter stabilization: do labile plant inputs form stable soil organic matter? Glob. Change Biol. 19 (4), 988–995. https://doi.org/10.1111/gcb.12113.
Dorrepaal, E., Toet, S., van Logtestijn, R.S.P., Swart, E., van de Weg, M.J., Callaghan, T.V., Aerts, R., 2009. Carbon respiration from subsurface peat accelerated by climate warming in the subarctic. Nature 460 (7255), 616–619 http://www.nature.com/nature/journal/v460/n7255/suppinfo/nature08216_S1.html.
Foley, J.A., Prentice, I.C., Ramankutty, N., Levis, S., Pollard, D., Sitch, S., Haxeltine, A., 1996. An integrated biosphere model of land surface processes, terrestrial carbon balance, and vegetation dynamics. Global Biogeochem. Cycles 10 (4), 603–628. https://doi.org/10.1029/96GB02692.
Gill, R.A., Polley, H.W., Johnson, H.B., Anderson, L.J., Maherali, H., Jackson, R.B., 2002. Nonlinear grassland responses to past and future atmospheric CO2. Nature 417 (6886), 279–282. https://doi.org/10.1038/417279a.
Hartley, I.P., Garnett, M.H., Sommerkorn, M., Hopkins, D.W., Fletcher, B.J., Sloan, V.L., et al., 2012. A potential loss of carbon associated with greater plant growth in the European Arctic. Nat. Clim. Change 2 (12), 875–879. https://doi.org/10.1038/nclimate1575.
Hobbie, S.E., Nadelhoffer, K.J., Högberg, P., 2002. A synthesis: the role of nutrients as constraints on carbon balances in boreal and arctic regions. Plant Soil 242 (1), 163–170. https://doi.org/10.1023/a:1019670731128.
Hofmockel, K.S., Zak, D.R., Moran, K.K., Jastrow, J.D., 2011. Changes in forest soil organic matter pools after a decade of elevated CO2 and O-3. Soil Biol. Biochem. 43 (7), 1518–1527. https://doi.org/10.1016/j.soilbio.2011.03.030.
Hoosbeek, M.R., Li, Y.T., Scarascia-Mugnozza, G.E., 2006. Free atmospheric CO2 enrichment (FACE) increased labile and total carbon in the mineral soil of a short rotation Poplar plantation. Plant Soil 281 (1–2), 247–254. https://doi.org/10.1007/s11104-005-4293-x.
Hungate, B.A., van Groenigen, K.J., Six, J., Jastrow, J.D., Luo, Y.Q., de Graaff, M.A., et al., 2009. Assessing the effect of elevated carbon dioxide on soil carbon: a comparison of

four meta-analyses. Glob. Change Biol. 15 (8), 2020–2034. https://doi.org/10.1111/j.1365-2486.2009.01866.x.
PCC, 2014: Climate Change 2014: Synthesis Report. Contribution of Working Groups I, II and III to the Fifth Assessment Report of the Intergovernmental Panel on Climate Change [Core Writing Team, R.K. Pachauri and L.A. Meyer (Eds.)]. IPCC, Geneva, Switzerland, 151 pp. (http://ar5-syr.ipcc.ch).
Korner, C., 2006. Plant CO2 responses: an issue of definition, time and resource supply. New Phytol. 172 (3), 393–411. https://doi.org/10.1111/j.1469-8137.2006.01886.x.
Kramshoj, M., Vedel-Petersen, I., Schollert, M., Rinnan, A., Nymand, J., Ro-Poulsen, H., Rinnan, R., 2016. Large increases in Arctic biogenic volatile emissions are a direct effect of warming. Nature Geosci. https://doi.org/10.1038/ngeo2692. advance online publication.
Kucharik, C.J., Foley, J.A., Delire, C., Fisher, V.A., Coe, M.T., Lenters, J.D., et al., 2000. Testing the performance of a dynamic global ecosystem model: water balance, carbon balance, and vegetation structure. Global Biogeochem. Cycles 14 (3), 795–825. https://doi.org/10.1029/1999GB001138.
Kuzyakov, Y., 2010. Priming effects: Interactions between living and dead organic matter. Soil Biol. Biochem. 42 (9), 1363–1371. https://doi.org/10.1016/j.soilbio.2010.04.003.
Lawrence, C.R., Neff, J.C., Schimel, J.P., 2009. Does adding microbial mechanisms of decomposition improve soil organic matter models? A comparison of four models using data from a pulsed rewetting experiment. Soil Biol. Biochem. 41 (9), 1923–1934 DOI 10.1016/j.soilbio.2009.06.016.
Lichter, J., Barron, S.H., Bevacqua, C.E., Finzi, A.C., Irving, K.E., Stemmler, E.A., Schlesinger, W.H., 2005. Soil carbon sequestration and turnover in a pine forest after six years of atmospheric CO2 enrichment. Ecology 86 (7), 1835–1847. https://doi.org/10.1890/04-1205.
Luo, Y.Q., Keenan, T.F., Smith, M., 2015. Predictability of the terrestrial carbon cycle. Glob. Change Biol. 21 (5), 1737–1751. https://doi.org/10.1111/gcb.12766.
Mahecha, M.D., Reichstein, M., Carvalhais, N., Lasslop, G., Lange, H., Seneviratne, S.I., et al., 2010. Global convergence in the temperature sensitivity of respiration at ecosystem level. Science 329 (5993), 838–840. https://doi.org/10.1126/science.1189587.
Moss, R.H., Edmonds, J.A., Hibbard, K.A., Manning, M.R., Rose, S.K., van Vuuren, D.P., et al., 2010. The next generation of scenarios for climate change research and assessment. Nature 463 (7282), 747–756. https://doi.org/10.1038/nature08823.
Norby, R.J., Warren, J.M., Iversen, C.M., Medlyn, B.E., McMurtrie, R.E., 2010. CO2 enhancement of forest productivity constrained by limited nitrogen availability. Proc. Natl. Acad. Sci. U.S.A. 107 (45), 19368–19373. https://doi.org/10.1073/pnas.1006463107.
Phillips, R.P., Meier, I.C., Bernhardt, E.S., Grandy, A.S., Wickings, K., Finzi, A.C., 2012. Roots and fungi accelerate carbon and nitrogen cycling in forests exposed to elevated CO2. Ecol. Lett. 15 (9), 1042–1049. https://doi.org/10.1111/j.1461-0248.2012.01827.x.
Quéré, C.L., Andrew, R.M., Canadell, J.G., Sitch, S., Korsbakken, J.I., Peters, G.P., et al., 2016. Global carbon budget 2016. Earth Syst. Sci. Data 8, 1–45. https://doi.org/10.5194/essd-8-1-2016.
Reynolds, L.L., Johnson, B.R., Pfeifer-Meister, L., Bridgham, S.D., 2015. Soil respiration response to climate change in Pacific Northwest prairies is mediated by a regional Mediterranean climate gradient. Glob. Change Biol. 21 (1), 487–500. https://doi.org/10.1111/gcb.12732.
Rousk, K., Michelsen, A., Rousk, J., 2016. Microbial control of soil organic matter mineralization responses to labile carbon in subarctic climate change treatments. Glob. Change Biol. 22 (12), 4150–4161. https://doi.org/10.1111/gcb.13296.
Schimel, J., 2013. SOIL CARBON Microbes and global carbon. Nat. Clim. Change 3 (10), 867–868. https://doi.org/10.1038/nclimate2015.
Shao, J., Zhou, X., Luo, Y., Zhang, G., Yan, W., Li, J., et al., 2016. Uncertainty analysis of terrestrial net primary productivity and net biome productivity in China during 1901–2005. J. Geophys. Res. Biogeosci. 121 (5), 1372–1393. https://doi.org/10.1002/2015jg003062.
Shi, Y., Xiang, X.J., Shen, C.C., Chu, H.Y., Neufeld, J.D., Walker, V.K., Grogan, P., 2015. Vegetation-associated impacts on Arctic Tundra bacterial and microeukaryotic communities. Appl. Environ. Microbiol. 81 (2), 492–501. https://doi.org/10.1128/Aem.03229-14.
Sistla, S.A., Moore, J.C., Simpson, R.T., Gough, L., Shaver, G.R., Schimel, J.P., 2013. Long-term warming restructures Arctic tundra without changing net soil carbon storage. Nature 497 (7451), 615-+. https://doi.org/10.1038/nature12129.
Sulman, B.N., Phillips, R.P., Oishi, A.C., Shevliakova, E., Pacala, S.W., 2014. Microbe-driven turnover offsets mineral-mediated storage of soil carbon under elevated CO2. Nat. Clim. Change 4 (12), 1099–1102. https://doi.org/10.1038/Nclimate2436.
Suseela, V., Conant, R.T., Wallenstein, M.D., Dukes, J.S., 2012. Effects of soil moisture on the temperature sensitivity of heterotrophic respiration vary seasonally in an old-field climate change experiment. Glob. Change Biol. 18 (1), 336–348. https://doi.org/10.1111/j.1365-2486.2011.02516.x.
Taylor, K.E., Stouffer, R.J., Meehl, G.A., 2012. An overview of CMIP5 AND the experiment design. Bull. Am. Meteorol. Soc. 93 (4), 485–498. https://doi.org/10.1175/bams-d-11-00094.1.
The-R-Core-Team, 2016. R: A Language and Environment for Statistical Computing, Vienna, Austria.
Todd-Brown, K.E.O., Randerson, J.T., Hopkins, F., Arora, V., Hajima, T., Jones, C., et al., 2014. Changes in soil organic carbon storage predicted by Earth system models during the 21st century. Biogeosciences 11 (8), 2341–2356. https://doi.org/10.5194/bg-11-2341-2014.
Trueman, R.J., Gonzalez-Meler, M.A., 2005. Accelerated belowground C cycling in a managed agriforest ecosystem exposed to elevated carbon dioxide concentrations. Glob. Change Biol. 11 (8), 1258–1271. https://doi.org/10.1111/j.1365-2486.2005.00984.x.
Trumbore, S., 2009. Radiocarbon and soil carbon dynamics. Annu. Rev. Earth Planet. Sci. 37, 47–66.
Voigt, C., Lamprecht, R.E., Marushchak, M.E., Lind, S.E., Novakovskiy, A., Aurela, M., et al., 2017. Warming of subarctic tundra increases emissions of all three important greenhouse gases – carbon dioxide, methane, and nitrous oxide. Glob. Change Biol. 23 (8), 3121–3138. https://doi.org/10.1111/gcb.13563.
Wang, G., Jagadamma, S., Mayes, M.A., Schadt, C.W., Steinweg, J.M., Gu, L., Post, W.M., 2015. Microbial dormancy improves development and experimental validation of ecosystem model. ISME J. 9 (1), 226–237. https://doi.org/10.1038/ismej.2014.120.
Wang, G.S., Post, W.M., Mayes, M.A., 2013. Development of microbial-enzyme-mediated decomposition model parameters through steady-state and dynamic analyses. Ecol. Appl. 23 (1), 255–272.
Wang, K., Peng, C., Zhu, Q., Zhou, X., Wang, M., Zhang, K., Wang, G., 2017. Modeling global soil carbon and soil microbial carbon by integrating microbial processes into the ecosystem process model TRIPLEX-GHG. J. Adv. Model. Earth Syst. https://doi.org/10.1002/2017ms000920.
Widder, S., Allen, R.J., Pfeiffer, T., Curtis, T.P., Wiuf, C., Sloan, W.T., et al., 2016. Challenges in microbial ecology: building predictive understanding of community function and dynamics. ISME J. 10 (11), 2557–2568. https://doi.org/10.1038/ismej.2016.45.
Wieder, W., 2014. Soil carbon: microbes, roots and global carbon. Nat. Clim. Change 4 (12), 1052–1053. https://doi.org/10.1038/nclimate2454.
Wieder, W.R., Bonan, G.B., Allison, S.D., 2013. Global soil carbon projections are improved by modelling microbial processes. Nat. Clim. Change 3 (10), 909–912 Doi 10.1038/Nclimate1951.
Zhou, J.Z., Deng, Y., Shen, L.N., Wen, C.Q., Yan, Q.Y., Ning, D.L., et al., 2016. Temperature mediates continental-scale diversity of microbes in forest soils. Nat. Commun. 7, 10. https://doi.org/10.1038/ncomms12083.
Zhu, Q., Liu, J., Peng, C., Chen, H., Fang, X., Jiang, H., et al., 2014. Modelling methane emissions from natural wetlands by development and application of the TRIPLEX-GHG model. Geosci. Model Dev. 7 (3), 981–999. https://doi.org/10.5194/gmd-7-981-2014.
Zhu, Q., Peng, C.H., Chen, H., Fang, X.Q., Liu, J.X., Jiang, H., et al., 2015. Estimating global natural wetland methane emissions using process modelling: spatio-temporal patterns and contributions to atmospheric methane fluctuations. Glob. Ecol. Biogeogr. 24 (8), 959–972. https://doi.org/10.1111/geb.12307.